Transnational University Limburg is a unique collaboration of two universities in two countries: the University of Hasselt and Maastricht University.

UHASSELT
KNOWLEDGE IN ACTION

www.uhasselt.be
Universiteit Hasselt
Campus Hasselt:
Martelarenlaan 42 | 3500 Hasselt
Campus Diepenbeek:
Agoralaan Gebouw D | 3590 Diepenbeek

UHASSELT
KNOWLEDGE IN ACTION

Maastricht University

Faculty of Medicine and Life Sciences
School for Life Sciences
Master of Biomedical Sciences

Master's thesis

Turning Back Time: Can Targeting Cellular Senescence Enhance Recovery After Spinal Cord Injury?

Yanne Van Reusel

Thesis presented in fulfillment of the requirements for the degree of Master of Biomedical Sciences, specialization Molecular Mechanisms in Health and Disease

SUPERVISOR :
Prof. dr. Helena SLAETS

MENTOR :
Mevrouw Naomi VEENINGEN

2023
2024

UHASSELT
KNOWLEDGE IN ACTION

Maastricht University

Faculty of Medicine and Life Sciences
School for Life Sciences
Master of Biomedical Sciences

Master's thesis

Turning Back Time: Can Targeting Cellular Senescence Enhance Recovery After Spinal Cord Injury?

Yanne Van Reusel

Thesis presented in fulfillment of the requirements for the degree of Master of Biomedical Sciences, specialization Molecular Mechanisms in Health and Disease

SUPERVISOR :

Prof. dr. Helena SLAETS

MENTOR :

Mevrouw Naomi VEENINGEN

Turning Back Time: Can Targeting Cellular Senescence Enhance Recovery After Spinal Cord Injury?*

Yanne Van Reusel[1], Naomi Veeningen[1], Niels Hellings[1] and Leen Slaets[1]

[1]Neuroimmune connections & repair lab, Biomedical Research Institute, Universiteit Hasselt, Campus Diepenbeek,
Agoralaan Building C - B-3590 Diepenbeek

**Targeting cellular senescence in spinal cord injury*

To whom correspondence should be addressed: Leen Slaets, Tel: +32(0)11 26 92 19; Email: Leen. slaets@uhasselt.be

Keywords: Spinal cord injury, fisetin, cellular senescence, flavonoid, aging

ABSTRACT

Background: Spinal cord injury (SCI) affects millions globally, with current treatments offering limited repair (1). Notably, the rising mean age coincides with increased activity of the elderly, possibly leading to traumatic SCI (2, 3). This population may have an increased predisposition to cellular senescence compared to younger individuals, potentially impairing recovery (4). Moreover, SCI itself induces senescence in younger individuals, suggesting its key role in impaired repair (5). Targeting cellular senescence emerges as a promising avenue to improve SCI recovery.

Methods: A mouse model was used to investigate the impact of aging on SCI recovery. Young (12 weeks) and old (18 months) mice received SCI via contusion. Functional recovery was evaluated for 28 days post-injury (dpi). Cellular senescence and expression of genes associated with aging and/or inflammation (p16, p21, IL-1α, IL-6, TGF-β, CXCL1, CCL2, 3 and 5) was investigated using immunohistochemistry and qPCR. Finally, fisetin, a senolytic compound, was administered to the same mouse model to assess its effect on functional recovery and senescence markers.

Results: Old mice displayed significantly poorer functional recovery and a higher mortality rate compared to young mice. qPCR revealed an increase in p16 expression following SCI. Fisetin administration did not improve functional recovery and did not reduce p16 expression.

Conclusion: Our study demonstrates that aging worsens functional recovery after SCI. These findings suggest that SCI worsens senescence and is increased compared to young SCI mice but cannot be reduced by fisetin.

INTRODUCTION

Approximately one million individuals worldwide suffer from **spinal cord injury (SCI)**, and yet current treatments are ineffective in repairing the spinal cord injury (1). SCI can result from a traumatic injury, such as a motor vehicle accident, or a non-traumatic injury, such as a spine tumor or infection. 90% of SCIs are caused by a traumatic injury, however the incidence of non-traumatic causes is rising (2). Notably, the mean age of SCI increases as the older population becomes more active, where 84% are caused by a traumatic injury such as a fall (3). These elderly may have a higher predisposition to **cellular aging**, hindering recovery or even leading to death (4). The primary injury causes damage to the spinal cord or surrounding tissues. After the primary injury, the immune system is known to play a key role in the secondary injury by aggravating this injury (6). In this phase, necrosis due to ischemia activates the infiltration of various immune cells, such as microglia, macrophages, polymorphonuclear cells, and lymphocytes, to the site of injury. Here, they will try to remove debris but actually aggravate the inflammation and further damage cells. Upon cell death, free radicals and glutamate are released and propagate the secondary injury cascade. After attempts of remyelination, a glial scar will be

formed and the lesion changes from a dynamic process to a chronic phase. Due to this complex interplay of many factors, such as immune cells, cytokines, and chemokines, up to now no significant advancements in biomedical research have enabled complete repair of the injury (6). Cellular senescence is discovered to be an influencing factor in various diseases, presenting a promising new approach for the development of future therapies aimed at enhancing SCI outcomes.

Aging of cells, known as **cellular senescence**, may play a crucial role in impairing the healing process of SCI (5). Senescent cells are distinct from other cells by their difference in the expression of certain molecules (7). These molecules are p16, p21, and SA-β-gal (7). p16 plays a role in cell cycle arrest, as it is upregulated in senescent cells; it causes inhibition of cyclin-dependent kinases 4/6 (CDK 4/6), which leads to a G1 cell cycle arrest. p21, on the other hand, is activated by p53, which is upregulated due to DNA damage because of telomere shortening (8). Lastly, upregulation of SA-β-gal indicates an increase in β-galactosidase activity, which is present in senescent cells (9). Endogenous beta-galactosidase (β-gal) is a lysosomal hydrolase able to break glycosidic bonds and thus plays an important role in energy production (10). It has maximum enzymatic activity at a pH of 4. On the contrary, SA-β-gal is characterized by chemical reactions at pH 6 (9). Paramos *et al.* have already demonstrated that SA-β-gal$^+$ cells are induced upon injury in the spinal cord (5). In total, these changes to senescent cells cause them to secrete pro-inflammatory factors and shift them to a senescence-associated secretory phenotype (SASP) and may cause aggravation of the injury (7).

However, it remains unclear how cellular senescence affects the differences observed in functional recovery between younger and older individuals with SCI. Underlying the functional gain of muscle usage, cellular senescence might play an important role. Older individuals are more likely to have a higher predisposition to senescence, which might lead to a higher pro-inflammatory state, ultimately leading to worse recovery. Hence, this pro-inflammatory environment might affect the functional recovery after SCI.

Fisetin, a flavonoid with a proven **senolytic** property, has emerged as a potential candidate for SCI treatment. Flavonoids are dietary compounds found in many fruits and vegetables and have an overall health-promoting effect (11). Senolytic drugs induce cell death, specifically in senescent cells, and clear them from the body. Since it is known that fisetin has fewer side effects compared to the current treatment, methylprednisolone, it might be a better therapy option. Methylprednisolone is known to have various severe adverse effects, emphasizing the need for an alternative therapy with minimal adverse effects (6, 12). Yousefzadeh *et al.* have already demonstrated that fisetin exhibits high senolytic activity on p16$^+$ T cells. This makes fisetin an ideal candidate for targeting senescence in SCI patients to improve outcomes (11). Therefore, fisetin is a promising therapeutic intervention that can reduce senescence and enhance the healing process by influencing the secondary injury cascade (5). However, despite research, the effect of fisetin on cellular senescence, its impact at the lesion site, and how this may improve SCI outcome remains unknown. Besides, this substance not only holds potential for SCI, but other pathologies related to aging, such as atherosclerosis and neurodegeneration.

Until now, research focused on the induction of cellular senescence after SCI without regard to the site of occurrence. This leaves many questions unanswered on how it influences SCI outcomes. Hence, this project aims to investigate the age-related differences in cellular senescence in female C57BL/6 mice with a contusion-induced SCI. Besides, fisetin, a potential treatment for immune aging in SCI is investigated. Based on previous research, we hypothesize that fisetin may reduce senescence through its senolytic property, thereby enhancing SCI recovery. Senescence typically increases as we age; thus, fisetin may enhance the recovery of SCI in elderly individuals through rejuvenation (5).

EXPERIMENTAL PROCEDURES

Animals – All animal experiments were handled in accordance with the local Ethical Committee and were carried out in compliance with the Belgian laboratory animal legislation and the European Communities Council Directive of 22 September 2010 (2010/63/EU). All experiments were performed with female C57BL/6 mice (Janvier) of 12 weeks and 17 months old.

Spinal cord injury contusion model - Mice were anesthetized using 2 – 3% Isoflurane

(IsofFlo, Abbot Animal Health) for induction and maximally 1.5% for maintenance. During surgery, T8 was identified based on anatomical landmarks such as blood vessels, followed by a laminectomy. The Infinite Horizon Impactor (Precision Systems & Instrumentation) induced a controlled force of 70 kdyne. This produced a consistent SCI model with a moderate to severe contusion. Afterward, the mice were allowed to recover from anesthesia in a recovery chamber at 33°C until they reached consciousness. The mice were checked for abnormalities in their hind limb movement after SCI induction. Post-operative care included glucose and Buprenorphine (0.1 mg/kg body weight). Buprenorphine is given up to 3 days post-injury (dpi). Baytril (Bayer) antibiotic was administered, and bladders were voided daily until they could urinate independently. If treated with fisetin, they received 100 mg/kg solved in corn oil (Thermo Fisher Scientific). 20% DMSO in corn oil was administered as a vehicle. The treatment was administered during two treatment periods. The first period starts at 2 dpi for five days and continues at 14 dpi for five days.

Behavioral testing – To assess the motor function of the hindlimbs, three behavioral tests were performed, starting from 0 dpi until 28 dpi for the Basso Mouse Scale (BMS) scoring, 7 dpi until 27 dpi for the rotarod tests, and 9 dpi until 25 dpi for the grip strength test.

The Basso Mouse Scale was used to assess functional recovery where a score of 0 resembles complete hind limb paralysis and 9 normal hind limb movement. Mice were put in an open field, and a score between 0 and 9 was assessed for each hind limb based on the observed hindlimb movement. For analysis, the mean of the right and left hind limbs was used.

Motor coordination and balance were tested with a rotarod test. Mice were put onto a rotating rod for a maximum time of 300 s with a gradually increasing speed of a maximum of 15 or 20 rpm. For each mouse, the time until fall was measured.

Grip strength was measured by placing the mouse onto a wire mesh cylinder with their forelimbs and held gently by their tail. Their hind paws were pulled over the grid, allowing the mouse to grab the metal grid. This was measured in maximum peak force by the grip strength meter (Conductor Science) and repeated three times. The mean of the three repeated measurements was used for further analysis.

Tissue collection and processing – Mice were sacrificed on day 28 post-injury by transcardiac perfusion under a lethal dose of Dolethal (Vetiquinol B.V.). Before perfusion, the spleen was removed, followed by cardiac puncture for blood collection and transcardial perfusion.

Immunohistochemistry (IHC) – Spinal cords of mice perfused with 4% PFA were frozen gradually in liquid nitrogen embedded in FSC 22 Frozen Section Media (Leica Biosystems). Afterward, the tissues were kept at -80°C until further processing. The spinal cords were cut into 10 µm thick sections on a cryostat (Leica CM3050 S, Leica) and mounted onto Superfrost Plus Adhesion Microscope Slides (Epredia). The tissue sections were blocked with 10% serum-free protein block (Dako, Agilent), and if needed, Ag-retrieval (HistoVT One, Nacalai Tesque) was performed. After permeabilization, primary antibodies were incubated overnight at 4°C. After washing, samples were incubated with the secondary antibodies for 1h at RT. The used antibodies (primary and secondary) can be found in supplemental (Table S1 and S2). Sections were washed and incubated with 4′,6-Diamidino-2 Phenylindole (DAPI). Finally, the slides were washed, whereafter they were mounted with Fluoromount-G™ Mounting Medium (Invitrogen, Thermo Fisher Scientific) and stored at -20°C.

Gene expression analysis – Spleen and spinal cord with and without lesion were extracted from mice. These tissues were instantly frozen in liquid nitrogen. Qiazol (Qiagen) was used to lyse the tissue, and RNA was isolated using an RNeasy Mini Kit (Qiagen), following the manufacturer's instructions, and cDNA was produced using qScript cDNA Supermix (Quanta Biosciences). This cDNA conversion was performed under the manufacturer's instructions. After finishing, the samples are kept at a temperature of 4°C until qPCR is continued.

qPCR – Primer pairs were designed for the following targets: p16, p21, IL-1α, IL-6, CXCL1, TGF-β, CCL2, CCL3, CCL5. Primer sequences can be found in supplemental (Table S3). Quantitative PCR was performed on the Quantstudio 3 (Thermo Fisher Scientific) according to the protocol for fast SYBR green. Data was normalized to the most stable

housekeeping genes (GAPDH, YWHAZ, CYPA, and HMBS), and stability was determined by GeNorm.

Imaging and data analysis – Whole slide images were acquired using the Axio Scan.Z1 Slide Scanner (ZEISS) using the Plan ApoChromat 40x/0.95 Corr M27 objective. Images were further processed using ZEISS ZEN Lite (Version 3.9) and ImageJ.

Statistics – Statistics were performed using GraphPad (Prism version 10.2.0). The data was checked for normal distribution (Shapiro-Wilk test) and outliers (ROUT test). Two-way ANOVA and Mixed-effect analysis with post-hoc Tukey test were performed. A P value of 0.05 was considered significant.

RESULTS

Functional recovery is impaired in old mice – A controlled contusion SCI was induced in young (3 months old) and old (17 months old) mice using a 70 kdyne impact force. To assess the influence of age on functional recovery, both groups were monitored for 28 dpi. Three functional evaluations were performed.

First, the Basso Mouse Scale (BMS) score (Fig. 1A) provides insights into locomotor function. This score revealed a significantly worse recovery in old mice from 12 dpi to 28 dpi (minimal P value < 0.05 and maximal P value < 0.0001) (13). By 28 dpi, the mean BMS score for old mice was 1.95, indicating extensive ankle movement. In contrast, young mice achieved a mean score of 2.7, signifying plantar placing of the paw with or without weight support or occasional, frequent, or consistent dorsal stepping (13).

Prior to surgery, all mice were trained on the rotarod treadmill to ensure that they were able to perform the task. Following SCI, SCI Old exhibited decreased performance on 9 dpi compared to SCI Young (Fig. 1B). Young SCI mice remained longer on the rotarod (242 seconds) compared to Old SCI mice (52 seconds) (minimally P value < 0.05 and maximally P value < 0.0001). This difference persisted until 22 dpi.

Finally, hindlimb grip strength measurements revealed a significant difference only at 9 dpi (P value < 0.0001) (Fig. 1C). Additionally, the mortality rate in old mice (40%) was higher than in young mice (10%) (Fig. 1D).

These findings demonstrate that old mice experience a worse recovery following SCI compared to young mice.

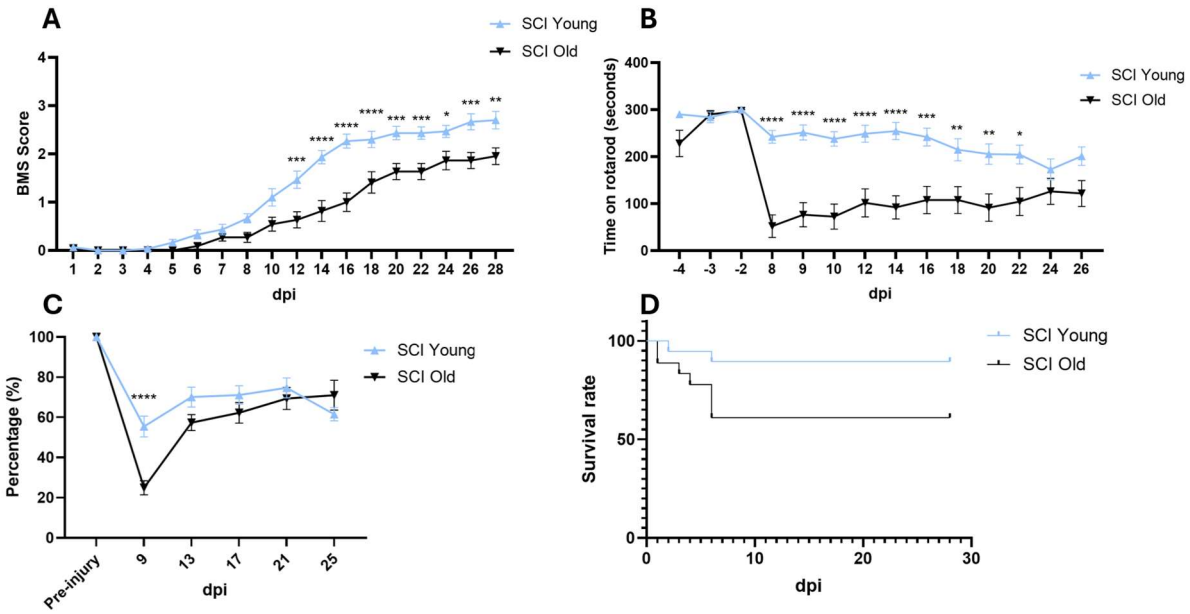

Fig. 1 – Old mice (18 months old) show worse recovery and a higher mortality rate compared to young mice (4 months old). A. BMS score was assessed at different time points post-injury until 28 dpi. Old SCI mice reduced functional recovery starting from 12 dpi until 28 dpi. **B.** Rotarod training is performed to ensure both age groups are able to perform the task. After SCI, both experimental groups experienced a decrease in seconds until fall. However, the time on rotarod of SCI old was significantly lower compared to SCI young. Differences were observed from 8 dpi until 22 dpi. **C.** Hind paw grip strength was assessed and only showed differences on 9 dpi. **D.** Old mice have a higher mortality after SCI. Data is shown as mean + SEM and a two-way anova or mixed-effect analysis with post-hoc Tukey test was performed. *: P value < 0.05, **: P value < 0.01, ***: P value < 0.001, and ****: P value < 0.0001.
SCI, Spinal Cord Injury; BMS, Basso Mouse Scale; dpi, days post-injury.

Age does not affect the astrocytic scar and demyelination – Since old mice exhibit poorer functional recovery compared to young mice following SCI, this study aimed to identify underlying differences responsible for this variation. Due to the applied force, a distinct lesion is induced, visualized by immunohistochemistry. The markers that were stained for are: glial fibrillary acidic protein (GFAP) and myelin basic protein (MBP).

GFAP identifies astrocytic scarring, a hallmark of the lesion site. The measured areas of the $GFAP^+$-region were comparable between young (2.14 mm^2) (Fig. 2B) and old mice (2.16 mm^2) (Fig. 2C), indicating no significant difference in scar formation (Fig. 2A).

MBP, on the other hand, detects myelin, a critical component for nerves and crucial for signal conduction. The measured areas of MBP^--regions, representing demyelination, were also not significantly different (Fig. 2D) between young (0.97 mm^2) (Fig. 2E) and old mice (1.11 mm^2) (Fig. 2F).

Our findings suggest that the size of the astrocytic scar and demyelination area may not be the primary factors contributing to the impaired recovery in old mice.

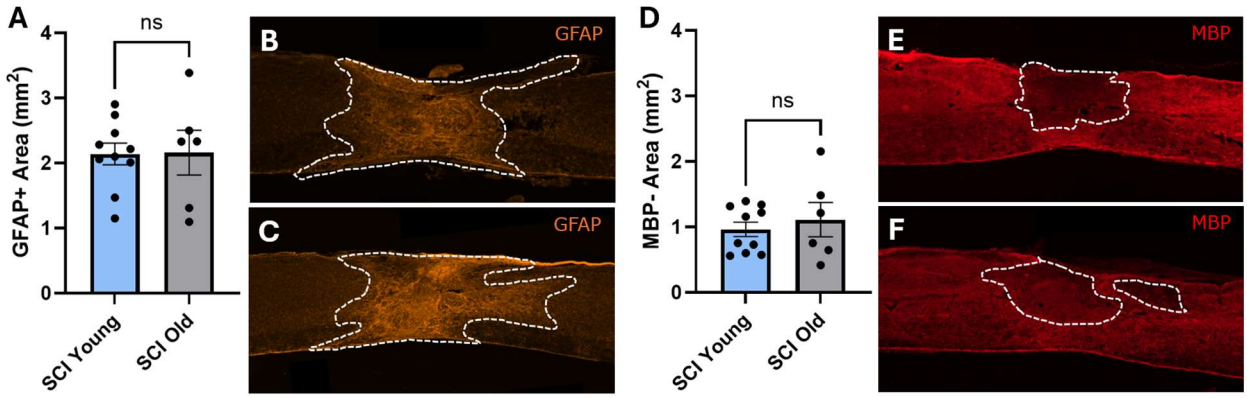

Fig. 2 – **The astrocytic scar and demyelination is not increased in old mice (18 month old) and are not responsible for differences observed in functional recovery. A.** Staining of GFAP visualizes the astrocytic scar. The area of the lesion was quantified and revealed no differences in lesion size between SCI young and SCI old. Representative images of GFAP staining of **B.** SCI young and **C.** SCI old. **D.** Besides GFAP, MBP was visualized which stains myelin. The lesion is characterized by loss of myelin and thus a negative signal for MBP. Quantification of MBP^--region showed no differences between SCI young and SCI old. Representative images of MBP staining of **E.** SCI young and **F.** SCI old. Data is shown as mean + SEM and an unpaired t test was performed.
Glial Fibrillary Acidic Protein, GFAP; Myelin Basic Protein, MBP; Spinal Cord Injury, SCI.

Senescent marker SA-beta-gal is increased after SCI, and is further increased by old age at injury – Next, we investigate the potential role of cellular senescence and if it increases post-SCI. SA-β-GAL, a lysosomal hydrolase active at a higher pH (pH 6) compared to endogenous β-galactosidase (pH 4), was used as a marker of cellular senescence.

Quantification of SA-β-GAL positive ($SA\text{-}\beta\text{-}GAL^+$) cells and corrected for the area (mm^2) within the gray matter revealed an increase in senescence due to SCI. While no statistically significant difference was observed between young (7.99 cells/mm^2) and old (54.57 cells/mm^2) healthy controls (Fig. 3B, E, and H), an upward trend in $SA\text{-}\beta\text{-}GAL^+$ cells was noted. Similarly, young SCI mice (73.46 cells/mm^2) displayed a slight increase (non-significant) in $SA\text{-}\beta\text{-}GAL^+$ cells compared to healthy controls (7.99 cells/mm^2). Importantly, old SCI mice exhibited a significantly higher number of $SA\text{-}\beta\text{-}GAL^+$ cells (219.0 cells/mm^2) (Fig. 3F, G, and H) compared to old healthy controls (54.57 cells/mm^2) and young SCI mice (73.5 cells/mm^2; P value < 0.001) (Fig. 3C, D, and H). This suggests a potential synergistic effect of age and SCI on cellular senescence.

Furthermore, analysis revealed distinct spatial patterns of senescence (Fig. 3I). In young SCI mice, no significant difference was observed between rostral (31.7 cells/mm^2) (Fig. 3C) and caudal (41.8 cells/mm^2) (Fig. 3D) regions to the lesion. However, old SCI mice showed a significant increase in rostral SA-β-GAL+ cells (61.7 cells/mm^2) (Fig. 3F) compared to caudal regions (39.8 cells/mm^2) (Fig. 3G). These findings demonstrate that SA-β-GAL is upregulated by SCI, with a rostral-caudal difference observed specifically in old animals.

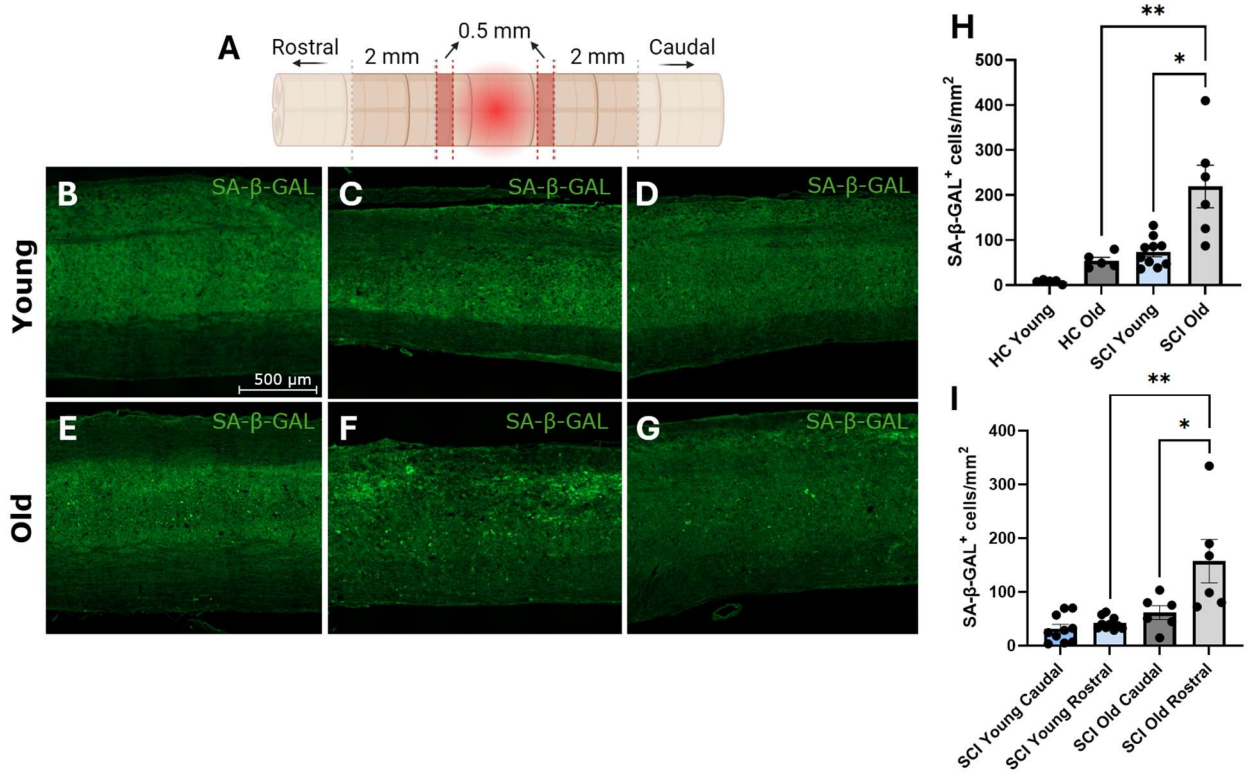

Fig. 3 – SA-β-GAL is induced by SCI. A. Schematic overview of analyzed sections. Starting from the border of the lesion, a zone of 0.5 mm was excluded. Following a region of 2 mm was analyzed, both rostrally and caudally to the lesion. **B.** Representative images of HC young, **C.** SCI young rostral, **D.** SCI young caudal, **E.** HC old, **F.** SCI old rostral, and **G.** SCI old caudal. **H.** Number of SA-β-GAL$^+$ cells/mm^2 in the spinal cord was increased after SCI in old mice (P value < 0.01). Additionally, there is a higher SA-β-GAL cell burden in old SCI mice in comparison to SCI young mice (P value <0.05). HC old shows no increase in SA-β-GAL$^+$ cells/mm^2 compared to HC young (P value: 0,7637) **I.** The amount of SA-β-GAL$^+$ cells/mm^2 caudally and rostrally to the lesion. SA-β-GAL$^+$ cells were increased rostral from the lesion in SCI old. This amount of SA-β-GAL$^+$ cells is significantly different from the rostral positive cells in SCI young. Data is shown as mean + SEM and a two-way anova was performed. *: P value < 0.05, **: P value < 0.01.
SCI, Spinal Cord Injury; SA-β-GAL, Senescence Associated beta-galactosidase.

P16 expression is increased post-SCI in old mice – While SA-β-GAL is a common marker for senescence, an additional marker is crucial to confirm cellular senescence. To address this, p16, a protein known to be upregulated during cellular senescence and to induce G1 cell cycle arrest via CDK4/6 inhibition, was used.

Gene expression analysis revealed an age-dependent response after SCI regarding p16. While young mice displayed no significant increase in p16 expression post-SCI, old mice showed a significant upregulation, particularly within the lesion area (1 cm with lesion centrally) compared to rostral-to-lesion (rostral from lesion area) areas and young SCI mice (Fig. 4A). p21, a downstream target of p53 signaling activated by DNA damage, displayed an upward trend with age and SCI (Fig. 4B).

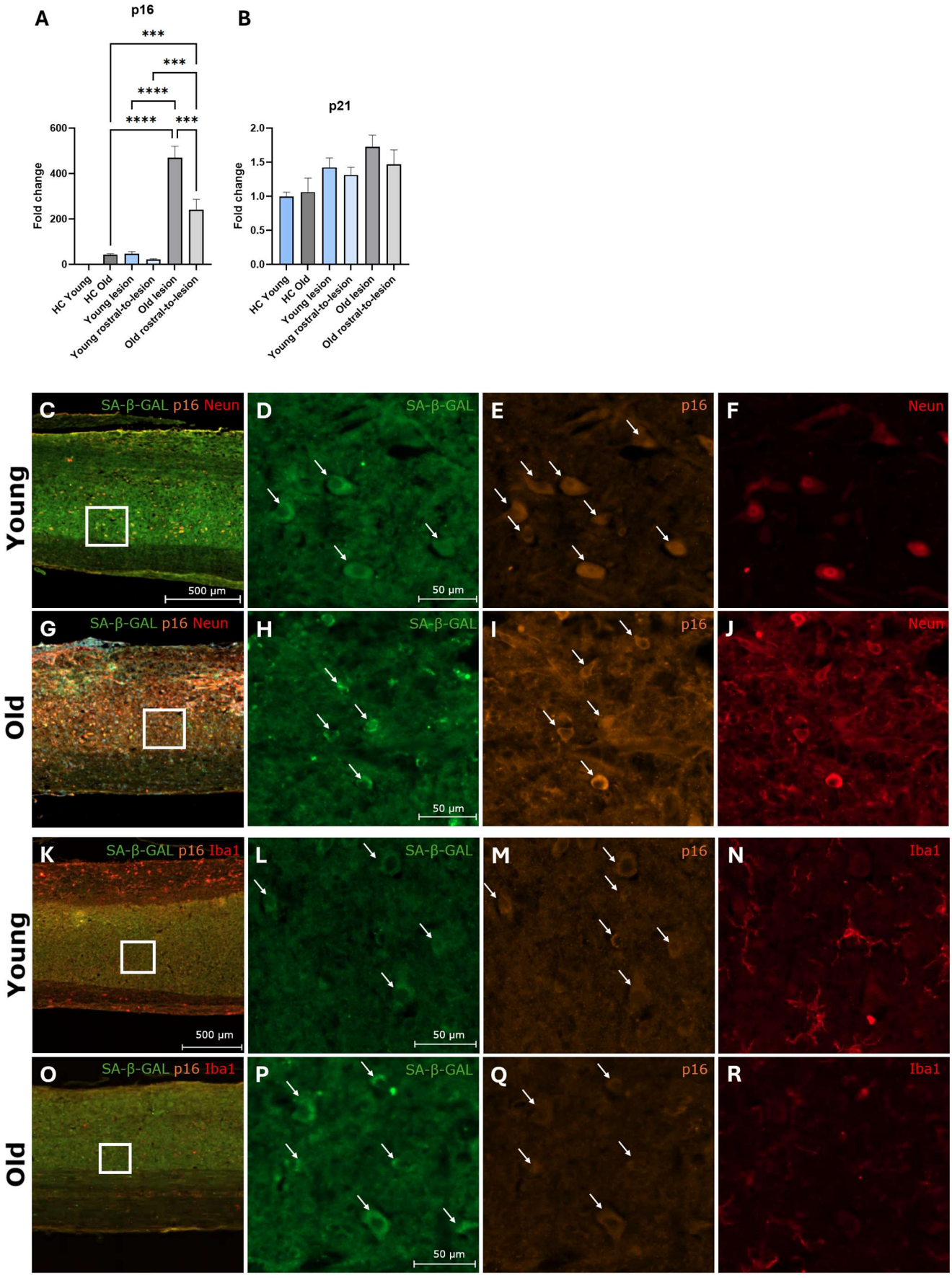
A
p16
***
***
****
****
***
600
400
200
0
Fold change
HC Young
HC Old
Young lesion
Young rostral-to-lesion
Old lesion
Old rostral-to-lesion
B
p21
2.0
1.5
1.0
0.5
0.0
Fold change
HC Young
HC Old
Young lesion
Young rostral-to-lesion
Old lesion
Old rostral-to-lesion
C
SA-β-GAL p16 Neun
500 µm
D
SA-β-GAL
50 µm
E
p16
F
Neun
Young
G
SA-β-GAL p16 Neun
H
SA-β-GAL
50 µm
I
p16
J
Neun
Old
K
SA-β-GAL p16 Iba1
500 µm
L
SA-β-GAL
50 µm
M
p16
N
Iba1
Young
O
SA-β-GAL p16 Iba1
P
SA-β-GAL
50 µm
Q
p16
R
Iba1
Old

Fig. 4 – After SCI, neurons show senescent characteristics, expression of SA-β-GAL and p16. SA-β-GAL is a senescence marker. However, p16 might be used to see if the SA-β-GAL$^+$ are in G1 cell cycle arrest. In addition, Neun and Iba1 provide a first glimpse on a cell type that might have senescent characteristics. **A.** p16 **B.** and p21 expressions were assessed using qPCR. p16 was upregulated after SCI in old mice in both lesion (P value<0.0001) and rostral-to-lesion (P value<0.001). On top of that, p16 was significantly (P value < 0.001) more abundant in the lesion than in the rostral-to-lesion of SCI old. After SCI, a significant increase of p16 in the lesion (P value<0.0001) and rostral-to-lesion (P value<0.001) of SCI old mice was observed compared to SCI young mice. On the contrary, no differences were observed in p21 expression. **C and K.** Merged overview image of the spinal cord of SCI young with zoomed in region highlighted. **D and L.** Representative image of SCI young SA-β-GAL, **E and M.** p16, and **F.** Neun. **G and O.** Merged overview image of the spinal cord of SCI old with zoomed in region highlighted. **H and P.** Representative image of SCI old SA-β-GAL, **I and Q.** p16, and **J.** Neun. **N and R.** Staining of Iba1 shows no overlap of SA-β-GAL and p16 with Iba1. Data is shown as mean + SEM and a two-way anova was performed. ***: P value < 0.001, and ****: P value < 0.0001.
SCI, Spinal Cord Injury; SA-β-GAL, Senescence Associated beta-galactosidase; Neun, neuronal nuclear protein; Iba1, ionized calcium-binding adapter molecule 1.

Neurons show cellular senescence after SCI – Immunohistochemistry confirmed p16 expression within the spinal cord. Co-staining of SA-β-GAL and p16 revealed an overlap in SCI mice (both young and old) (Fig. 4D, E, L, M, P, and Q), suggesting that SA-β-GAL$^+$ cells are also undergoing G1 arrest and thus may be senescent. Furthermore, co-localization with Neun (Fig. 4C-F and G-J), a neuronal marker, demonstrated that neurons displayed markers for senescence after SCI. Conversely, the absence of co-localization with Iba1 (Fig. 4K-N, and O-R), a microglial marker, indicated that microglia, do not undergo senescence due to SCI. Additionally, some cells did show senescence (SA-β-GAL$^+$ and p16$^+$) but did not stain for Neun (Fig. S2).

Together, this confirms the presence of cellular senescence in spinal cord neurons following SCI.

SASP is induced following SCI and contributes to chronic inflammation – Cellular senescence was observed caudally and rostrally from the lesion site with the use of immunohistochemistry stainings. SA-β-GAL and p16 were often colocalized with Neun, and thus, neurons displayed a senescent phenotype. Senescent cells are known to exhibit SASP, characterized by the secretion of pro-inflammatory factors like interleukin-1α (IL-1α), transforming growth factor-β (TGF-β), and CXCL1, potentially hindering the healing process. However, it remains unknown if SASP is induced following SCI.

The investigated genes, IL-1α, IL-6, CXCL1, TGF-beta, CCL2, CCL3, and CCL5, are all members of SASP (Table 1). qPCR analysis revealed a significant upregulation of IL-1α within the lesion area following SCI in both young and old mice compared to healthy controls (Fig. 5) at 28 dpi. Furthermore, IL-1α displayed significantly higher expression within the lesion compared to the rostral-to-lesion spinal cord (young P value < 0.01; old P value < 0.001). An additional upregulation in the rostral-to-lesion area of young SCI mice compared to their healthy counterparts (P value < 0.05) was observed. In contrast, no significant changes were observed in IL-6 expression.

CXCL1 mirrored the pattern of IL-1α, increased expression within the lesion compared to their healthy control (P value < 0.0001) or rostral-to-lesion part (P value < 0.0001) in young and old mice. However, it did not show an increased expression in the rostral-to-lesion part of young SCI mice compared to young HC.

Interestingly, TGF-β expression not only increased significantly within the lesion following SCI (P value < 0.0001) but also demonstrated an age-dependent effect post-SCI, with old SCI mice exhibiting higher levels compared to young SCI mice (P value < 0.05).

CCL2 and CCL5 showed increased expression within the lesion compared to their healthy control (P value < 0.0001) or rostral-to-lesion part (P value < 0.0001) in young and old mice.

Similarly, CCL3 expression displayed a significant increase within the lesion (P value < 0.0001) and upregulation in the rostral-to-lesion area of old SCI mice compared to controls (P value < 0.05).

These findings suggest that SCI induces the expression of SASP markers, including IL-1α, CXCL1, CCL2, and CCL5. Additionally, TGF-β expression appears to be influenced by both SCI and age. The observed presence of

cellular senescence and the SASP phenotype in old mice after SCI may contribute to their poorer functional recovery. Given the potential role of senescence, senolytic drugs could be explored as a therapeutic strategy to improve functional outcomes.

Table 1 – Investigated cytokines by qPCR and how they are affected by SASP.

Cytokine	Secreted by	Immune cells recruited	Sources
IL-1α	Macrophages, dendritic cells, fibroblasts, endothelial cells, keratinocytes, and hepatocytes	Macrophages and neutrophils	(14)
IL-6	Macrophages, endothelial cells, and T cells	Macrophages, neutrophils, and T-cells	(14)
CXCL1	Neutrophils, macrophages and epithelial cells,	Neutrophils, monocytes, and macrophages	(15)
TGF-β	Parenchymal, lymphocytes, monocytes, macrophages, and platelets	Neutrophils	(16, 17)
CCL2	Monocytes and macrophages	Monocytes, memory T lymphocytes, and natural killer (NK) cells.	(18)
CCL3	Mononuclear phagocytes, lymphocytes, NK cells, endothelium, fibroblasts, epithelial cells, and mesothelium	Monocytes, lymphocytes, eosinophils, and basophils	(19)
CCL5	T cells, macrophages, activated platelets, endothelial cells, and vascular smooth muscle cells	T-cells, eosinophils, and monocytes	(20, 21)

Changes that occur with cellular senescence in genes related to SASP. The investigated cytokines are increased in SASP (16, 22). IL-1α, Interleukin 1α; IL-6, Interleukin 6; CXCL1, Chemokine (C-X-C motif) ligand 1; CCL2, C-C motif chemokine ligand 2; CCL3, C-C motif chemokine ligand 3; CCL5, C-C motif chemokine ligand 5.

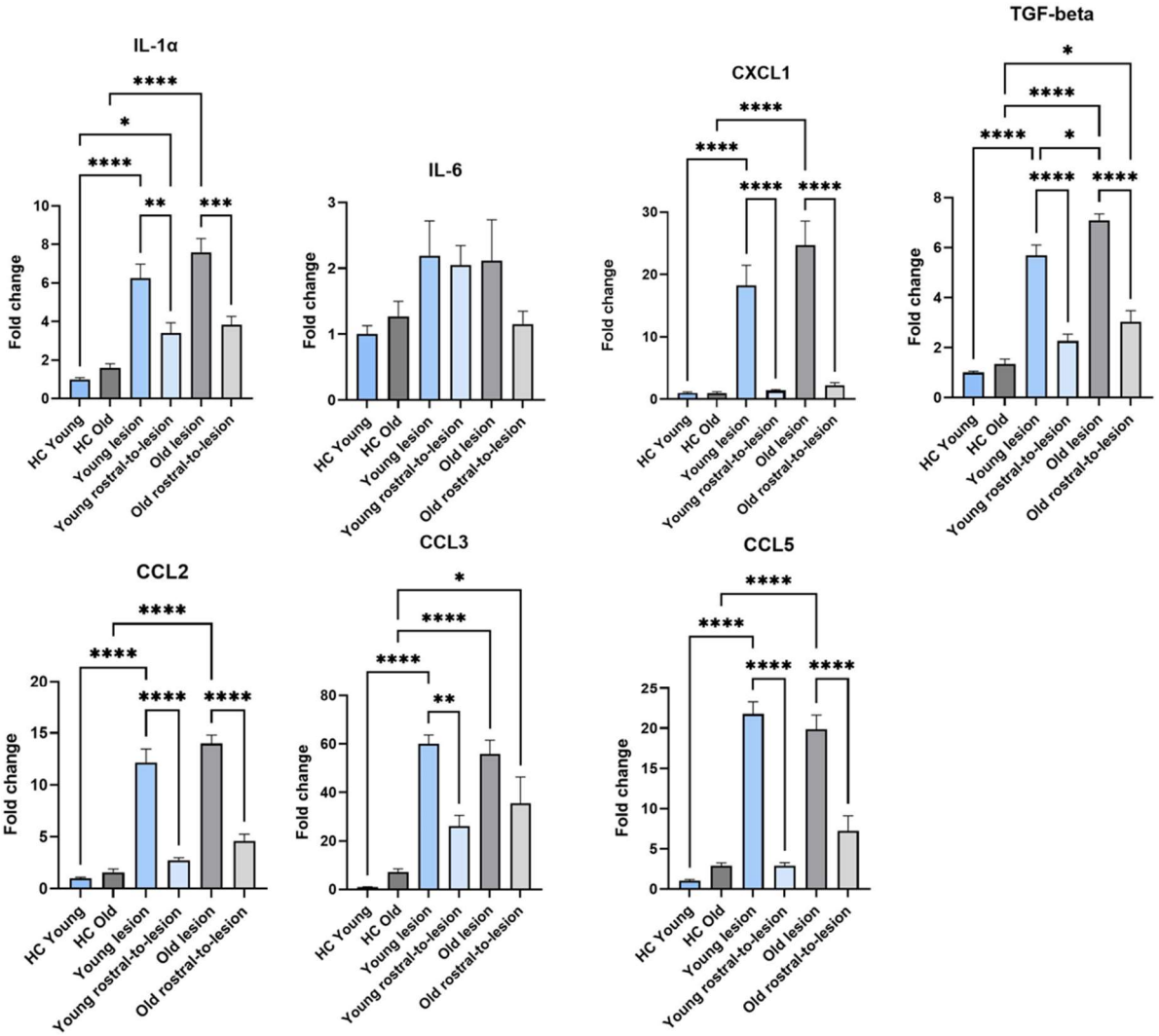

Fig. 5 – Worse functional recovery might be influenced by SASP induction post-SCI. Gene expression was assessed using qPCR for the chosen targets: IL-1α, IL-6, CXCL1, TGF-beta, CCL2, CCL3, and CCL5 were determined in healthy controls and SCI. In SCI, lesion and rostral-to-lesion gene expression was evaluated. Normalized for CYPA and HMBS. Data is shown as mean + SEM and a two-way anova was performed. *: P value < 0.05, **: P value < 0.01, ***: P value < 0.001, and ****: P value < 0.0001.
IL-1α, Interleukin 1α; IL-6, Interleukin 6; CXCL1, Chemokine (C-X-C motif) ligand 1; TGF-β, Transforming growth factor beta; CCL2, C-C motif chemokine ligand 2; CCL3, C-C motif chemokine ligand 3; CCL5, C-C motif chemokine ligand 5.

Functional recovery is not improved by fisetin administration – Fisetin, a senolytic compound known to eliminate senescent cells, was administered based on that it could improve functional recovery after SCI by reducing the senescent cell burden observed in figure 3 and 4. Following a "hit-and-run" regimen, fisetin was administered for five days, starting at 2 dpi and 14 dpi, targeting both pre-existing and SCI-induced senescent cells.

However, functional recovery assessments using BMS (Fig. 6A) and rotarod (Fig. 6B) did not reveal any differences between the fisetin-treated groups and vehicle. While the rotarod test successfully distinguished between young and old mice, with older animals exhibiting a reduced time until fall, fisetin administration did not improve performance in either age group.

Furthermore, increased mortality rate of old mice (Fig. 6C) was observed compared to old mice of figure 1D. As the first treatment period began at 2 dpi, deaths prior to this point cannot be attributed to the treatment itself.

Despite the lack of functional improvement observed with fisetin treatment

(Fig. 6), the effect on p16 expression was further investigated. A sustained age-dependent increase in p16 expression in both lesion and rostral-to-lesion was revealed, consistent with previous findings (Fig. 4K). Disappointingly, fisetin administration did not result in a decrease in p16 expression compared to vehicle, suggesting that the current protocol may not be effective in eliminating senescent cells in this model.

Collectively, these findings suggest that fisetin administration, following the current protocol, does not improve functional recovery after SCI.

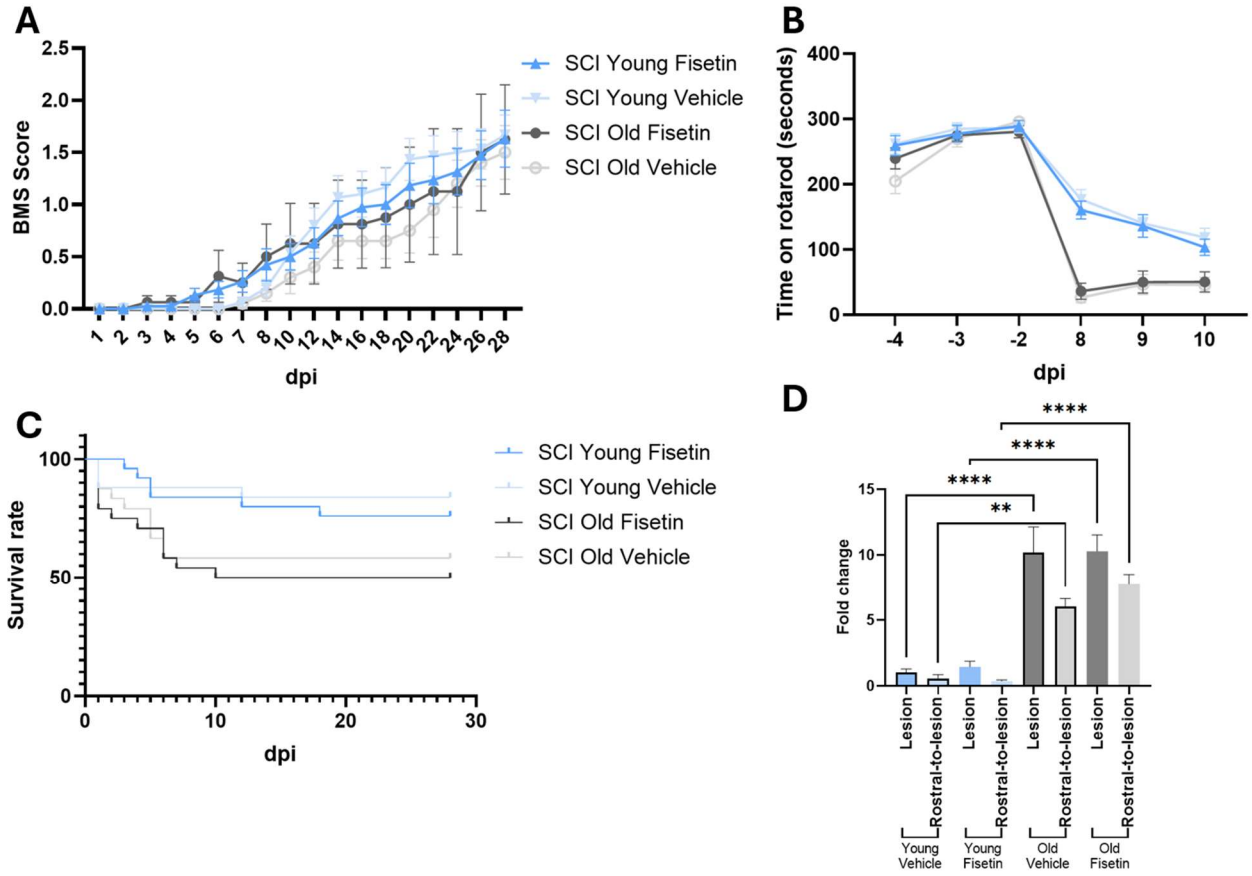

Fig. 6 – Fisetin shows no effect on functional recovery after SCI. A. BMS score was assessed at different time points post-injury until 28 dpi. No differences were observed. A 5-day treatment period started on 2 dpi and 14 dpi. Fisetin treatment had a dose of 100 mg/kg, and the vehicle contained 20% DMSO. **B.** Rotarod training is performed to ensure both age groups are able to perform the task. After SCI, experimental groups experienced a decrease in seconds until fall. However, the time on rotarod of each SCI old group was lower compared to their SCI young mice. Differences were observed from 7 dpi to 21 dpi. At 27 dpi, the SCI young vehicle is higher compared to the SCI old Vehicle. **C.** Old mice have a higher mortality after SCI. **D.** Fisetin (100 mg/kg) was administered to young and old SCI mice, administration did not reduce p16 expression. Additionally, the age-associated increase of p16, as in Figure 4A, was observed. Normalized for CYPA and HMBS. Data is shown as mean + SEM, and a two-way ANOVA was performed. *: P value < 0.05, **: P value < 0.01, ***: P value < 0.001, and ****: P value < 0.0001.
SCI, Spinal Cord Injury; BMS, Basso Mouse Scale; dpi, days post-injury.

DISCUSSION

Cellular senescence, characterized by G1 cell cycle arrest and impaired proliferation, is a key contributor to impaired post-SCI recovery. Various events, including oxidative stress, reactive metabolites, and DNA damage, all of which are prevalent following SCI, can induce senescence (23). In this study, we observed a correlation between increased cellular senescence and worse functional recovery in old mice after SCI. This finding aligns with the concept of SASP. SASP is characterized by the secretion of pro-inflammatory factors that can create a persistent chronic low-grade inflammatory state and hinder tissue repair (5).

Our data suggests a potential link between aging and a higher predisposition to cellular senescence. The observed worse functional recovery in old mice compared to young mice, as evidenced by significant differences in BMS scores, rotarod performance (starting at 8 dpi, $P < 0.0001$), and grip strength, could be attributed to a pre-existing higher burden of senescent cells and to a more pronounced induction of senescence post-injury in old animals. Our findings on increased mortality in old mice post-SCI are consistent with Takano *et al.* who reported a mortality rate of 10% in young mice and 35% in old mice and further support this finding. In conclusion, our results strongly suggest that an increase in cellular senescence in response to injury is responsible for the worse recovery observed in old SCI mice.

Our investigation revealed a significant difference in functional recovery between young and old mice post-SCI. While lesion size is often implicated in such difference, no significant differences were observed in our study, aligning with findings from Kumamaru *et al.* who employed mice with an age range of 4 week vs. 10 week-old mice but at various time points after SCI. 10 weeks is considered as mature adult but still a young age. Interestingly, Takano *et al.* reported a larger lesion size in old mice at 9 dpi (early sub-acute phase) using mice more similar to our study (2-3 months vs. 15-18 months). This study used neurofilament-200 (NF200) besides GFAP. NF200 is used to stain neurofilament and is a marker for axons. A decrease in NF200 is correlated to axonal loss (24). This suggests a potential influence of the evaluation timepoint on lesion size, as scar formation typically is completed at 28 dpi in our model, potentially masking underlying differences. Further investigation is crucial to explore other potential mechanisms.

Our findings suggest that cellular senescence may be a key contributor to the diminished functional recovery observed in old mice following SCI. SA-β-GAL, a well-established marker of cellular senescence, was not significantly elevated in the uninjured old mice compared to HC Young. However, a marked increase in SA-β-GAL$^+$ cell burden was observed in SCI Old compared to both HC Old and SCI Young mice. Furthermore, immunohistochemistry revealed a distinct higher senescent cell burden rostrally from the lesion in SCI Old mice, suggesting potential heterogeneity in the senescent cell pattern. This aligns with the concept of diverse SASP programs proposed by Paramos *et al.*, where specific SASP profiles could differentially impact tissue repair. Rhinn *et al.* suggest that inducing cellular senescence has beneficial effects in various situations, such as tumor suppression, development, and regeneration. It is important that this senescence is tightly regulated to have beneficial effects. If not, SASP will accumulate and cause inflammation of the tissue. Senescent cells will secrete SASP and can induce senescence in cells via a paracrine route. In this way, cellular senescence is spreaded to neighbouring cells and spreading throughout the tissue (25).

The observed difference in SA-β-GAL spatial distribution between young and old SCI mice suggests that age-related alterations by cellular senescence may contribute to worse functional recovery in old animals (5, 26).

P21 and p16 are besides SA-β-GAL, two senescent cell markers. P16 and p21 play a role in cell cycle arrest, as they are upregulated in senescent cells and cause inhibition of cyclin-dependent kinases. p21, is activated by p53, which is upregulated due to DNA damage because of telomere shortening. It has a role in inducing cellular senescence. p16, on the other hand, causes inhibition of cyclin-dependent kinases 4/6 (CDK 4/6), which leads to a permanent G1 cell cycle arrest (8). An increase of p16 expression in the lesional area was observed compared to the rostral non-lesion area, indicating the same distinct spatial pattern of cellular senescence as observed in SA-β-GAL. p21 did not show differences after SCI or due to aging. Immunohistochemistry showed that SA-β-GAL often colocalizes with p16 indicating that cells with SA-β-GAL also are present in G1 cell cycle arrest and stopped dividing. P16 expression

is associated with persistent senescence as it increases with age and blocks cyclin-dependent kinases, which causes permanent cell-cycle arrest (5, 27). Additionally, Neun and Iba1 were used to determine whether SA-β-GAL and p16 colocalize and, thus, which cell became senescent. Neurons showed colocalization indicating that these neurons show a senescent phenotype after SCI. This was not only observed in SCI Old mice but also in SCI Young mice. Microglia did not colocalize with p16 and/or SA-β-GAL. However, microglia sometimes surrounded cells positive for SA-β-GAL or p16 (Fig. S1). Some cells showed staining for SA-β-GAL and p16 but did not stain for Neun (Fig. S2). This indicates that other cell types besides neurons and microglia may have a role in the cellular senescence observed. Rivellini *et al.* and Zhang *et al.* both investigated cellular senescence in oligodendrocytes. Rivellini *et al.* and Zhang *et al.*, have explored cellular senescence in oligodendrocytes (28, 29). After SCI, oligodendrocyte precursor cells (OPCs) are recruited to initiate the remyelination process (30). However, these OPCs may undergo senescence, a state characterized by irreversible replicative arrest and impaired functionality. This senescence compromises their proliferative capacity and ability to produce myelin sheaths, thereby hindering effective remyelination and functional recovery (28, 29). Taken together, these findings suggest that cellular senescence is abundantly present in the spinal cord and show that neurons are senescent after SCI.

SASP, the secretion of pro-inflammatory factors, associated with cellular senescence, can create a persistent chronic low-grade inflammatory state and hinder tissue repair (5). In this study, we investigated the expression of several SASP markers, including interleukin-1α (IL-1α), interleukin-6 (IL-6), chemokine (C-X-C motif) ligand 1 (CXCL1), transforming growth factor beta (TGF-β), C-C motif chemokine ligand 2 (CCL2), CCL3, and CCL5. While IL-1α and IL-6 are known to activate the immune response, in SASP, they will maintain chronic inflammation, potentially synergistically with other SASP factors (31-34). CXCL1 can have beneficial effects like clearing damaged cells, but dysregulation leads to chronic inflammation (33). TGF-β possesses both pro- and anti-inflammatory properties, promoting tissue repair but also inhibiting cell proliferation and contributing to fibrosis at high concentrations (16). Fibrosis is a consequence of severe tissue damage when complete regeneration is not possible. In such instances, dysregulated wound healing processes lead to uncontrolled deposition of extracellular matrix (ECM) components, ultimately leading to scar formation. A key player in this pathological process is TGF-β. Studies by López-Otín *et al.* have demonstrated an association between abnormal upregulation of TGF-β and the development of fibrosis-associated diseases. Their findings suggest that following SCI, known to trigger fibrosis, elevated levels of TGF-β contribute to lesion formation. Additionally, the observation of higher TGF-β levels in the lesions of older SCI mice compared to young SCI mice suggests a potential link between age and exacerbated fibrosis following SCI. Similarly, CCL2, CCL3, and CCL5, also known as MCP-1, MIP-1α, and RANTES, respectively, play a role in healing but can exacerbate chronic inflammation in the context of SASP (35, 36). Importantly, our data revealed no significant increases in SASP markers due to healthy aging alone. However, a significant upregulation of most SASP markers, except for IL-6, was observed at the lesion site of SCI mice compared to their healthy counterparts or rostral to the lesion. Cui *et al.* found that IL-6 is upregulated at 28 dpi in rats (37). Another study by Segal *et al.* found elevated levels of IL-6 in their plasma (38). These findings suggest that SCI triggers a robust SASP response, potentially contributing to the chronic inflammation observed in both young and old mice after injury.

Our findings support the involvement of cellular senescence in the impaired functional recovery observed after SCI. This highlights the potential of targeting senescent cells as a therapeutic strategy. Fisetin, a senolytic compound, has shown promise in previous studies by Cui *et al.* and Yousefzadeh *et al.* (11, 37). The second study indicated a reduction of senescent cells in various tissues and suppression of age-related pathologies (11). Additionally, Cui *et al.* have revealed the neuroprotective properties of fisetin administered orally in SCI through modulation of the NF-κB/IκBα pathway (37). This leads to decreased pro-inflammatory and apoptotic mediators and increased neurotrophic factors, resulting in improved outcomes in rats (37). We used a "hit-and-run" treatment regimen with fisetin administered via oral gavage for five consecutive days, starting at 2 dpi and continuing at 14 dpi. However, this approach did not significantly improve functional recovery or reduce p16 expression in either young or old mice

compared to the vehicle group. Additionally, no differences were observed between Young and old SCI mice. Several factors might explain the lack of efficacy observed with fisetin in our study. The chosen administration route (oral gavage) could be a contributing factor. Previous studies report the effectiveness of fisetin's senolytic effects via oral administration. Due to translation to human use, oral administration is preferred. However, fisetin has a low bioavailability and is less soluble in aqueous solutions. Kumar *et al.* tried to solve these problems and developed a self-nano-emulsifying drug delivery system (SNEDDS) for fisetin. This strategy involves solving fisetin within an oil using surfactants and co-surfactants. Upon administration, the formulation converts into a nanoemulsion and thereby enhancing absorption and bioavalilability of fisetin. They found that this way of administration improved bioavailability (39). By employing this delivery system we can increase the bioavailability and still use the preferred route of administration. If this might not provide the desired effects, intraperitoneal injection can be explored as another option (11, 37, 40, 41). Additionally, the significant stress response associated with SCI and its experimental procedures, particularly in old mice, could potentially diminish fisetin's effectiveness. Further investigation using alternative administration routes and stress reduction strategies is warranted to definitively assess fisetin's therapeutic potential in this context.

CONCLUSION

This study investigated the role of cellular senescence in functional recovery after SCI. Our findings strongly suggest that cellular senescence is a key contributor to the impaired functional recovery observed in old mice. Increased cellular senescence, as observed by immunohistochemistry of SA-β-GAL and gene expression of p16, correlated with worse functional outcomes in old mice compared to young mice.

Furthermore, our data suggests that SCI triggers a robust SASP pattern, potentially contributing to the chronic inflammation observed in both young and old mice. While fisetin, a senolytic compound, has shown promise in other studies, our current "hit-and-run" administration regimen did not improve functional recovery or reduce the senescent marker, p16.

Future studies should explore the optimization of administration or alternative administration routes and stress reduction strategies to definitively assess the therapeutic potential of targeting cellular senescence for improved functional recovery after SCI. We believe that fisetin or another potent senolytic might provide beneficial effects in the recovery of SCI. It may not have the potential to replace other current therapies, but it might have great potential to work synergistically alongside other therapies in SCI.

REFERENCES

1. Ding W, Hu S, Wang P, Kang H, Peng R, Dong Y, et al. Spinal Cord Injury: The Global Incidence, Prevalence, and Disability From the Global Burden of Disease Study 2019. Spine (Phila Pa 1976). 2022;47(21):1532-40.
2. WHO. Spinal cord injury [Available from: https://www.who.int/news-room/fact-sheets/detail/spinal-cord-injury.
3. Ikpeze TC, Mesfin A. Spinal Cord Injury in the Geriatric Population: Risk Factors, Treatment Options, and Long-Term Management. Geriatr Orthop Surg Rehabil. 2017;8(2):115-8.
4. Groah SL, Charlifue S, Tate D, Jensen MP, Molton IR, Forchheimer M, et al. Spinal cord injury and aging: challenges and recommendations for future research. Am J Phys Med Rehabil. 2012;91(1):80-93.
5. Paramos-de-Carvalho D, Martins I, Cristovao AM, Dias AF, Neves-Silva D, Pereira T, et al. Targeting senescent cells improves functional recovery after spinal cord injury. Cell Rep. 2021;36(1):109334.
6. Ahuja CS, Wilson JR, Nori S, Kotter MRN, Druschel C, Curt A, et al. Traumatic spinal cord injury. Nat Rev Dis Primers. 2017;3:17018.
7. Yue Z, Nie L, Zhao P, Ji N, Liao G, Wang Q. Senescence-associated secretory phenotype and its impact on oral immune homeostasis. Front Immunol. 2022;13:1019313.
8. Kumari R, Jat P. Mechanisms of Cellular Senescence: Cell Cycle Arrest and Senescence Associated Secretory Phenotype. Front Cell Dev Biol. 2021;9:645593.
9. Valieva Y, Ivanova E, Fayzullin A, Kurkov A, Igrunkova A. Senescence-Associated beta-Galactosidase Detection in Pathology. Diagnostics (Basel). 2022;12(10).
10. Bioquest A. What is the primary function of β-galactosidase? 2020 [Available from: https://www.aatbio.com/resources/faq-frequently-asked-questions/What-is-the-primary-function-of-beta-galactosidase.
11. Yousefzadeh MJ, Zhu Y, McGowan SJ, Angelini L, Fuhrmann-Stroissnigg H, Xu M, et al. Fisetin is a senotherapeutic that extends health and lifespan. EBioMedicine. 2018;36:18-28.
12. Chikuda H, Yasunaga H, Takeshita K, Horiguchi H, Kawaguchi H, Ohe K, et al. Mortality and morbidity after high-dose methylprednisolone treatment in patients with acute cervical spinal cord injury: a propensity-matched analysis using a nationwide administrative database. Emerg Med J. 2014;31(3):201-6.
13. Basso DM, Fisher LC, Anderson AJ, Jakeman LB, McTigue DM, Popovich PG. Basso Mouse Scale for locomotion detects differences in recovery after spinal cord injury in five common mouse strains. J Neurotrauma. 2006;23(5):635-59.
14. ABBAS. Basic Immunology. sixth edition ed.
15. Wu CL, Yin R, Wang SN, Ying R. A Review of CXCL1 in Cardiac Fibrosis. Front Cardiovasc Med. 2021;8:674498.
16. Tominaga K, Suzuki HI. TGF-beta Signaling in Cellular Senescence and Aging-Related Pathology. Int J Mol Sci. 2019;20(20).
17. Branton MH, Kopp JB. TGF-beta and fibrosis. Microbes Infect. 1999;1(15):1349-65.
18. Deshmane SL, Kremlev S, Amini S, Sawaya BE. Monocyte chemoattractant protein-1 (MCP-1): an overview. J Interferon Cytokine Res. 2009;29(6):313-26.
19. Good. Neonatal Pulmonary Host Defense. 2017.
20. Costa RM, Cerqueira DM, Bruder-Nascimento A, Alves JV, Awata WAC, Singh S, et al. Role Of The C-C Motif Chemokine Ligand 5 (CCL5) And Its Receptor, C-C Motif Chemokine Receptor 5 (CCR5) In The Genesis Of Aldosterone-induced Hypertension, Vascular Dysfunction, And End-organ Damage. bioRxiv. 2023.
21. Uniprot. CCL5 [Available from: https://www.uniprot.org/uniprotkb/P13501/entry .
22. Coppe JP, Desprez PY, Krtolica A, Campisi J. The senescence-associated secretory phenotype: the dark side of tumor suppression. Annu Rev Pathol. 2010;5:99-118.
23. Zhang L, Pitcher LE, Yousefzadeh MJ, Niedernhofer LJ, Robbins PD, Zhu Y. Cellular senescence: a key therapeutic target in aging and diseases. J Clin Invest. 2022;132(15).
24. Torsney C, Anderson RL, Ryce-Paul KA, MacDermott AB. Characterization of sensory neuron subpopulations selectively expressing green fluorescent protein in phosphodiesterase 1C BAC transgenic mice. Mol Pain. 2006;2:17.
25. Rhinn M, Ritschka B, Keyes WM. Cellular senescence in development, regeneration and disease. Development. 2019;146(20).
26. Takano M, Kawabata S, Shibata S, Yasuda A, Nori S, Tsuji O, et al. Enhanced Functional Recovery from Spinal Cord Injury in Aged Mice after Stem Cell Transplantation

through HGF Induction. Stem Cell Reports. 2017;8(3):509-18.
27. Muss HB, Smitherman A, Wood WA, Nyrop K, Tuchman S, Randhawa PK, et al. p16 a biomarker of aging and tolerance for cancer therapy. Transl Cancer Res. 2020;9(9):5732-42.
28. Rivellini C, Porrello E, Dina G, Mrakic-Sposta S, Vezzoli A, Bacigaluppi M, et al. JAB1 deletion in oligodendrocytes causes senescence-induced inflammation and neurodegeneration in mice. J Clin Invest. 2022;132(3).
29. Zhang P, Kishimoto Y, Grammatikakis I, Gottimukkala K, Cutler RG, Zhang S, et al. Senolytic therapy alleviates Abeta-associated oligodendrocyte progenitor cell senescence and cognitive deficits in an Alzheimer's disease model. Nat Neurosci. 2019;22(5):719-28.
30. Huntemer-Silveira A, Patil N, Brickner MA, Parr AM. Strategies for Oligodendrocyte and Myelin Repair in Traumatic CNS Injury. Front Cell Neurosci. 2020;14:619707.
31. Mariotti M, Castiglioni S, Bernardini D, Maier JA. Interleukin 1 alpha is a marker of endothelial cellular senescent. Immun Ageing. 2006;3:4.
32. Sapochnik M, Fuertes M, Arzt E. Programmed cell senescence: role of IL-6 in the pituitary. J Mol Endocrinol. 2017;58(4):R241-R53.
33. Ortiz-Montero P, Londono-Vallejo A, Vernot JP. Senescence-associated IL-6 and IL-8 cytokines induce a self- and cross-reinforced senescence/inflammatory milieu strengthening tumorigenic capabilities in the MCF-7 breast cancer cell line. Cell Commun Signal. 2017;15(1):17.
34. Frisch SM. Interleukin-1alpha: Novel functions in cell senescence and antiviral response. Cytokine. 2022;154:155875.
35. Baba T, Mukaida N. Role of macrophage inflammatory protein (MIP)-1alpha/CCL3 in leukemogenesis. Mol Cell Oncol. 2014;1(1):e29899.
36. Luciano-Mateo F, Cabre N, Baiges-Gaya G, Fernandez-Arroyo S, Hernandez-Aguilera A, Elisabet Rodriguez-Tomas E, et al. Systemic overexpression of C-C motif chemokine ligand 2 promotes metabolic dysregulation and premature death in mice with accelerated aging. Aging (Albany NY). 2020;12(20):20001-23.
37. Cui J, Fan J, Li H, Zhang J, Tong J. Neuroprotective potential of fisetin in an experimental model of spinal cord injury: via modulation of NF-kappaB/IkappaBalpha pathway. Neuroreport. 2021;32(4):296-305.
38. Segal JL, Gonzales E, Yousefi S, Jamshidipour L, Brunnemann SR. Circulating levels of IL-2R, ICAM-1, and IL-6 in spinal cord injuries. Arch Phys Med Rehabil. 1997;78(1):44-7.
39. Kumar R, Kumar R, Khurana N, Singh SK, Khurana S, Verma S, et al. Enhanced oral bioavailability and neuroprotective effect of fisetin through its SNEDDS against rotenone-induced Parkinson's disease rat model. Food Chem Toxicol. 2020;144:111590.
40. Liao YR, Lin JY. Quercetin intraperitoneal administration ameliorates lipopolysaccharide-induced systemic inflammation in mice. Life Sci. 2015;137:89-97.
41. Ren Q, Guo F, Tao S, Huang R, Ma L, Fu P. Flavonoid fisetin alleviates kidney inflammation and apoptosis via inhibiting Src-mediated NF-kappaB p65 and MAPK signaling pathways in septic AKI mice. Biomed Pharmacother. 2020;122:109772.

Acknowledgements – YVR expresses sincere gratitude to NV for exceptional guidance and support throughout this internship and research project. NV's feedback and expertise were important in all aspects of the work. YVR also extends appreciation to NV and Professor LS for taking the time to meticulously review and provide insightful comments on the thesis. YVR is grateful to the Healthy Aging Team and the NIC&R Team for offering the opportunity to delve into the fascinating field of cellular senescence in spinal cord injury research. YVR acknowledges the entire staff at BIOMED for their continuous support and training in practical laboratory techniques. YVR is particularly thankful to fellow students for their collaborative spirit, especially for their assistance in troubleshooting data processing issues and brainstorming potential explanations for the findings. Finally, YVR expresses heartfelt thanks to everyone who provided encouragement and support during the thesis writing journey, no matter how big or how small their support was.

Author contributions – NV conceptualized and designed the research project. YVR and NV collaboratively conducted the experiments. NV ensured proper training on the utilized techniques for YVR. YVR performed the data analysis under the guidance NV. YVR drafted the thesis, incorporating the valuable feedback provided by NV and Professor LS.

SUPPLEMENTAL

Table S1 – Primary antibodies

Target	Concentration used	Manufacturer
rat anti-MBP	1:250	Millipore, MAB386
mouse anti-GFAP	1:200	Sigma-Aldrich, G3893
mouse anti-Neun	1:1000	Millipore, MAB377
goat anti-IBA1	1:250	Abcam, ab107159

Table S2 – Secondary antibodies

Target	Concentration used	Manufacturer
goat anti-rat Alexa647	1:250	Invitrogen, A21247
goat anti-mouse Alexa568	1:250	Invitrogen, A11004
goat anti-mouse Alexa 647	1:250	Invitrogen, A21235

Table S3 – qPCR primers (forward and reverse)

Target	Forward	Reverse
p21	GTGATGTCCGACCTGTTCCG	CCACGGGACCGAAGAGACAA
p16	TCGTACCCCGATTCAGGTGAT	TAGTGGGGTCCTCGCAGTT
IL-6	TACCACTTCACAAGTCGGAGGC	CTGCAAGTGCATCATCGTTGTTC
TGF-β	GGGCTACCATGCCAACTTCTG	GAGGGCAAGGACCTTGCTGTA
CCL2 (MCP-1)	CAGCAGGTGTCCCAAAGAAG	CATTTGGTTCCGATCCAGGTT
CCL3 (MIP-1α)	GACTATTTTGAAACCAGCAGCCTTT	GATCTGCCGGTTTCTCTTAGTCA
CCL5 (RANTES)	GGAGTATTTCTACACCAGCAGCAA	TGTCACTCGAAGGAACCGC
IL-1α	AACCCATGATCTGGAAGAGACC	AAACTTCTGCCTGACGAGCTT
CXCL1	GGAGTATTTCTACACCAGCAGCAA	TGTCACTCGAAGGAACCGC

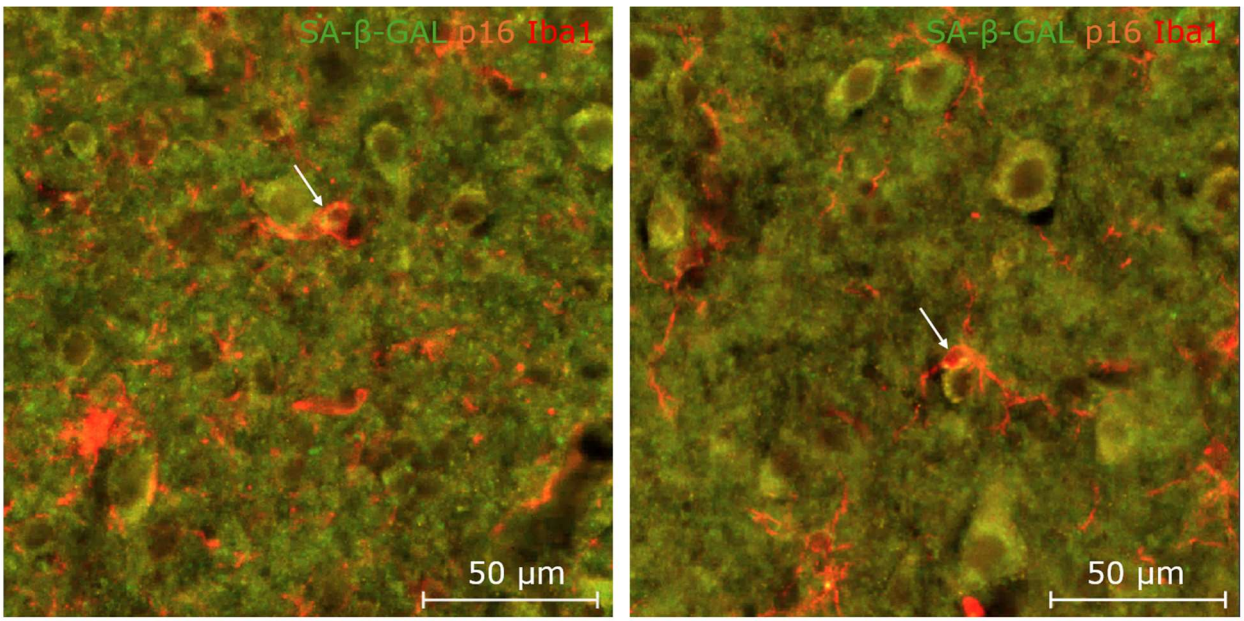

Fig. S1 – Microglia surround SA-β-GAL and p16 positive cells. Microglia showed to surround senescent cells (SA-β-GAL$^+$ and p16$^+$). Shown images show microglia neighbouring senescent cells indicated by an arrow.

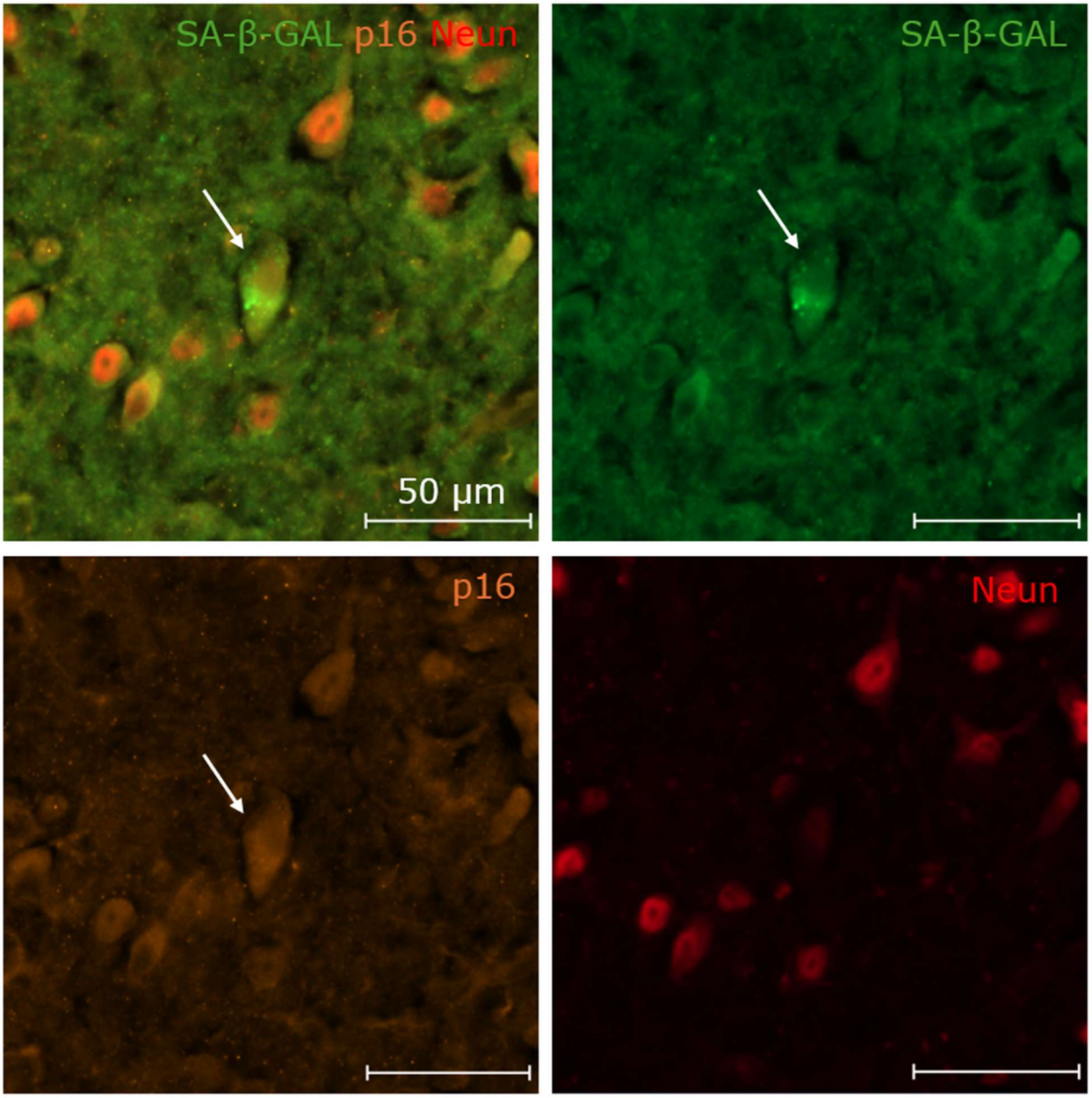

Fig. S2 – Senescent cells positive for SA-β-GAL and p16 show no overlap with Neun. Cells show senescent characteristics by positive signal for SA-β-GAL and p16. This indicates that these cells are in G1 cell cycle arrest and produce SA-β-GAL. However, staining for Neun shows no signal in a cell with senescent characteristics (indicated by the arrow).